Sensitivity Calibration of a Dual-Beam Vertically Pointing FM-CW Radar[1]

E. STRATMANN[2] AND D. ATLAS

Dept. of Geophysical Sciences, The University of Chicago

AND J. H. RICHTER AND D. R. JENSEN

Naval Electronics Laboratory Center, San Diego, Calif.

(Manuscript received 4 May 1971, in revised form 6 July 1971)

ABSTRACT

A method of calibrating a fixed vertically pointing radar is presented. The technique involves the firing of B-B shot of known radar cross section through the beam while making successive trajectory corrections until the absolute maximum signal is attained. The results agree closely with an independent calibration of antenna gain. The approach is particularly suited to an FM-CW radar with high range resolution because the pellets reach heights well in excess of the minimum range and errors in range are negligible. Corrections are presented for the reduction in maximum two-way gain resulting from intersecting beams whose full gain is attained only at the point of intersection. It is also shown that Probert-Jones' k^2 factor is significantly smaller for this system, and possibly for others, than the generally accepted value of unity. The method can be readily extended to any sufficiently sensitive pulsed radar by using small elevation angles and direct measurements of range rather than those obtained from the echoes.

1. Introduction

The ultra high-resolution FM-CW radar designed by one of us (Richter, 1969) has been employed at the Naval Electronics Laboratory Center (NELC), San Diego, in studies of the fine-scale structure of the atmosphere through backscatter from refractively perturbed clear air strata. One of the most striking findings of these observations is that the scatter layers are often very thin, sometimes only a meter or less and rarely more than 30 m, but their peak reflectivities are commonly 10–10^2 times as large as the largest previously reported by Atlas and Hardy (1966) and Hardy and Katz (1969) [see Richter (1969) and Atlas *et al.* (1970)b]. The maximum reflectivity observed to date is 3×10^{-11} cm^{-1}, some 10^3 times as large as the greatest 10.7-cm value noted by Hardy and Katz. Because such reflectivities imply the existence of exceedingly large fluctuations in refractive index in thin strata which have only rarely been observed directly (Lane, 1968; Atlas *et al.*, 1970b), the importance of an accurate calibration of the overall system sensitivity became evident. This paper describes the calibration techniques. It is extracted from a more comprehensive report by Stratmann *et al.* (1971), hereinafter referred to as I.

Because the FM-CW radar is comprised of separate vertically pointing antennas for transmission and reception, both sunk below ground level and shielded by absorbing fences for purposes of isolation (Richter, 1969), it was not possible to use normal standard targets or an ordinary antenna range for calibration purposes. Indeed, while we tried to suspend a small spherical target from a tethered balloon within the beam, this proved unsuccessful. We therefore resorted to the use of a B-B pistol capable of firing 0.44-cm spherical copper pellets to heights of about 140 m. The method proved to be simple, cheap and accurate, and is recommended to those facing similar problems.

2. Theory

The bistatic[3] radar equation for a point target (Skolnik, 1970) is

$$P_r=\frac{P_tG_tA_r}{(4\pi r^2)^2}\sigma L\psi, \tag{1}$$

where P_r is the echo power, P_t the transmitted power, G_t the axial gain of the transmitting antenna, A_r the collection area of the receiving antenna, L the fractional total loss in the system and transmission path, σ the target cross section, and r its range. For our purposes, the most important assumption is that the target is on the intersection of the axes of both the transmitting and

[1] This paper is an extract from a more comprehensive report by the same title and authors (see references).

[2] On leave from the Research Institute of the German Post Office, Darmstadt, Germany.

[3] For antennas as closely spaced as those in the present radar, Eq. (1) is essentially the monostatic case with σ equal to the backscatter cross section.

receiving beams. The correction factor ψ, derived below, accounts for the reduction in two-way maximum gain resulting from the use of two intersecting beams. The effective antenna gain along the beam axis is

$$G_e = fG_m, \tag{2a}$$

$$G_e = f4\pi A/\lambda^2, \tag{2b}$$

where λ is the wavelength, f the antenna efficiency factor, $G_m = 4\pi A/\lambda^2$ is the maximum possible axial gain with $f=1$, and A the geometric area of the antenna. Note also that fA may be considered the effective collecting area of the antenna. Since the transmitting and receiving antennas are identical, (2a) and (2b) apply to both and Eq. (1) may then be expressed as

$$P_r = \frac{P_t\lambda^2(G_m^2 f^2 L)}{(4\pi)^3 r^4}\sigma\psi. \tag{3}$$

Because λ is known, and P_r, P_t and r are measurable, the use of a target having a known cross section σ effectively provides a measure of the parenthetical product in the numerator of (3). The radiation patterns and gains of the individual antennas were measured prior to installation but it was believed necessary to check the system sensitivity in the final configuration.

The main lobes of the radiation patterns measured at 2.90 GHz are shown in Fig. 1 for both antennas out to about $\pm 4°$ off the beam axis. We have superimposed the E (vertical polarization) and H (horizontal polarization) plane patterns of the main lobe of each antenna on an expanded scale for comparison. Also plotted are Gaussian patterns corresponding to half-power beam widths of 2.5°. We see that both the E and H patterns closely approximate the 2.5° Gaussian beam down to the -8 dB points below which the E patterns become narrower and the H patterns broader. The complete radiation patterns presented in I show that the first side lobes are greatly suppressed, especially in the E plane, so that the second side lobes in that plane are stronger. The side lobe suppression accounts in part for the relatively low antenna efficiencies and wide beams as discussed subsequently. The antenna gains at 2.9 GHz were measured as 35.4 and 35.2 dB for dishes 1 and 2, respectively. The half-power beamwidths are 2.5° for both antennas in both planes.

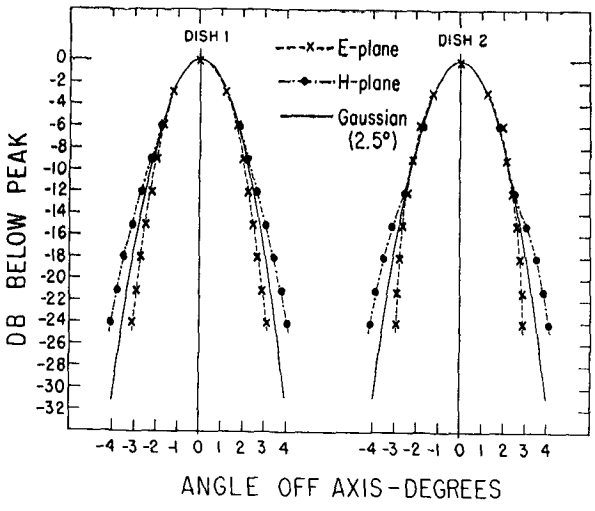

FIG. 1. Main lobe radiation patterns of the two antennas at 2.90 GHz. The E and H plane patterns are superimposed and compared to a Gaussian pattern of 2.5° half-power width.

In order to use (3) for purposes of calibration with a standard target, it is desirable that the target be in the far zone of the antennas because the effective axial gains are well defined only in that zone, or when $r \gtrsim 2D^2/\lambda$, where D is the antenna diameter. Silver (1949) notes, however, that the axial gain is reduced by no more than 6% when $r \gtrsim D^2/\lambda$. For the NELC system with both dish diameters equal to 3.05 m and the mid-wavelength of 10.35 cm, $D^2/\lambda = 89.9$ m. Since the B-B's generally attained heights in excess of 120 m, no correction is necessary for near-zone effects.

However, some correction may be necessary because of the tilting of the beams whose axes intersect at a height of 280 m. In actual fact, one beam is vertical and the other is canted at 1°; but we have treated the problem as if the beams were tilted toward each other by 0.5° from the vertical. The beam geometry is illustrated in Fig. 2 in a vertical plane between dish centers. The angles are exaggerated for clarity. This problem has been treated by Atlas *et al.* (1970a) and is summarized here in a slightly different form.

If we express the one-way illumination or gain pattern of the main lobe of the antenna as a Gaussian function of θ and ϕ, where θ is the angle relative to the beam axis in the section shown and ϕ the angle normal thereto, the two-way radiation pattern is the product of the two. Thus,

$$I(\theta_1,\phi_1,\theta_2,\phi_2) = \exp\left\{-\frac{1}{2}\left[\frac{\theta_1^2}{\sigma_{\theta_1}^2}+\frac{\phi_1^2}{\sigma_{\phi_1}^2}\right]\right\} \times \exp\left\{-\frac{1}{2}\left[\frac{\theta_2^2}{\sigma_{\theta_2}^2}+\frac{\phi_2^2}{\sigma_{\phi_2}^2}\right]\right\}, \tag{4}$$

where θ_1 and ϕ_1 are the angular coordinates of the target with respect to the transmitting beam axis, and similarly for θ_2 and ϕ_2 relative to the receiving beam axis. Also, $\sigma_\theta = \theta_h/(2\ln 2)^{\frac{1}{2}} = 0.849\theta_h$, where θ_h is half the beam width between half-power points, and similarly for σ_ϕ. When the antennas are co-located, the maximum of (4) is unity. We wish now to evaluate the reduction in maximum two-way gain resulting from separation of the antennas. Since we are concerned only with the maximum two-way illumination along the $\phi_1=\phi_2=0$ axis, the exponentials in (4) involving ϕ_1 and ϕ_2 are unity.

We may now express the angles θ_1 and θ_2 in terms of the horizontal distances x_1 and x_2 from their respective

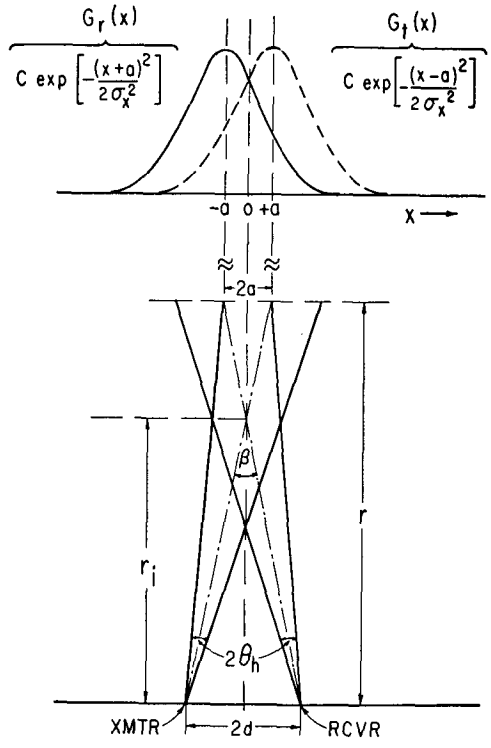

FIG. 2. Schematic diagram of the dual-beam configuration with beam axes interesecting at height $r_i=280$ m. At any height r, the two-way pattern is a product of the two patterns illustrated at the top. In actual fact, the transmitting beam is vertical and the receiving beam is tilted by 1° from the vertical. See text for details.

beam axes at a range r making use of the small angle relationships, $x_1=r\theta_1$, $x_2=r\theta_2$ and $\sigma_x=\sigma_\theta r$. In addition, we may express x_1 and x_2 in terms of the common coordinates from the vertical center line. Thus $x_1=x+a$ and $x_2=x-a$, indicating that the transmitting and receiving beam axes are centered at $x=+a$ and $x=-a$ relative to the common origin, where $2a$ is the horizontal distance between beam centers at range r. Note that above the height r_i of beam intersection the two beam axes reverse their positions relative to the origin, but this is of no concern because of symmetry. With the above substitutions the combined radiation pattern of Eq. (4) along $y=\phi_1 r=\phi_2 r=0$ finally reduces to

$$I(x, y=0)=\exp\left(-\frac{x^2}{\sigma_x^2}\right)\exp\left(-\frac{a^2}{\sigma_x^2}\right), \tag{5}$$

where

$$a=d|(1-r/r_i)|, \tag{6}$$

$2d$ is the spacing between the dish centers, and, because the antennas are identical, $\sigma_{x_1}=\sigma_{x_2}=\sigma_x$. This shows that the composite beam along the x direction is also a Gaussian centered at $x=0$, but with variance twice that of the individual beams and a maximum two-way gain (at $x=0$) reduced by ψ equal to the second exponential factor on the right of (5). In decibels, the reduction factor is

$$10\log_{10}\psi=-4.343(a/\sigma_x)^2, \tag{7a}$$

$$=-6.02\left(\frac{d}{\theta_h r_i}\right)^2\left(\frac{r_i}{r}-1\right)^2. \tag{7b}$$

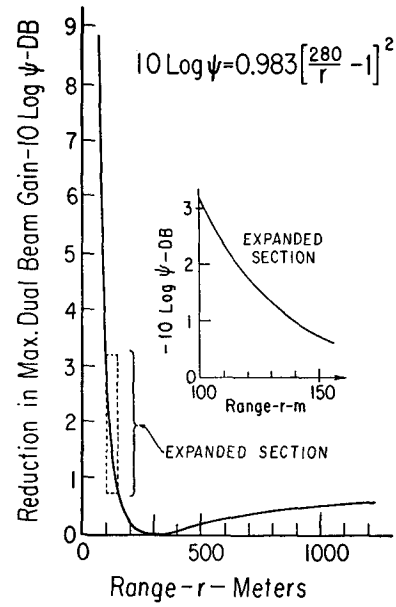

FIG. 3. Reduction in maximum two-way gain as a function of range due to offset in beam axes.

Eq. (7b) may be expressed in terms of β, the angle of beam intersection, by noting that $\beta=2d/r_i$. Eq. (7) is plotted in Fig. 3 for the NELC radar configuration with $d=2.435$ m, $r_i=280$ m, $\beta=1.01°$, and $2\theta_h=2.50°$. The inset is an expanded portion for the range interval 100–150 m, the heights reached by the B-B's.

When both beams are vertical and parallel to one another as in the case of the AN/TPQ-11 cloud detection radar, $a=d$ independent of height and $r_i=\infty$. Then the dB reduction factor is

$$10\log\psi=-6.02(d/r\theta_h)^2 \text{ [parallel beams]}. \tag{8}$$

3. Experiments

Taking 10 log [Eq. (3)] and subtracting the dB correction factor of (7), we obtain

$$10\log(P_r)=K-40\log r-0.983\left(\frac{280}{r}-1\right)^2, \tag{9}$$

where P_r is in milliwatts, r is in meters,

$$K=10\log[P_t G_m^2 f^2\lambda^2 L\sigma/(4\pi)^3] \text{ dB}>1 \text{ mW m}^4, \tag{10}$$

P_t is the transmitted power in milliwatts, λ is in meters and σ is in meters squared.

The values of the radar parameters in (10) are given in Table 1.

TABLE 1. Radar characteristics for the NELC FM-CW radar.

Transmitted power P_t: maximum	1.5×10^5 mW
typical	1.0×10^5 mW
in B-B tests	8.7×10^4 mW
Mid-wavelength λ	10.35 cm
Antennas	
Diameter D	3.048 m
Geometrical area A	7.295 m^2
Theoretical maximum gain G_m (at full efficiency)	8.57×10^3
Measured gain G_e	3.47×10^3*
Overall efficiency f	0.405*
Beamwidth $2\theta_h = 2\phi_h$	2.5°*
Dish separation 2d (center to center)	4.87 m
Height of beam intersection r_i	280 m
Losses (coax cables) L	0.5

* Antenna range measurements.

The B-B's used in the calibration were measured to have a radius of 0.2202 cm$\pm$0.85%. The radar cross section of such a small metal sphere is given by Kerr (1951) as

$$\sigma = 1.403 \times 10^4 \pi a^6/\lambda^4. \quad (11)$$

Thus, $\sigma = 4.38 \times 10^{-8}$ m$^2 \pm 5\%$.

During the 1970 experiments, a total of 77 B-B's were shot essentially vertically from a CO_2-powered B-B pistol positioned midway between the antennas. The pistol was mounted on the barrel of a theodolite to permit small corrections to be made for the effects of wind. Our goal was to shoot enough B-B's so that at least a few would cross the combined beam axis near the apex of their trajectory. This was further assured by small adjustments in the pistol orientation after each shot until we observed the maximum possible signals. The signals were recorded on magnetic tape, later reproduced on an oscilloscope, and photographed. Signal amplitudes on the scope were calibrated immediately following the shots by coupling a portion of the measured transmitted power into the receiver through a delay line and a set of precision attenuators. This has the advantage of eliminating any absolute error in the power measurement. The delayed and attenuated transmitter signal also provides a precision height marker at 187 m range. A second delayed pulse appears at a range of 167 m, thereby providing an accurate range scale.

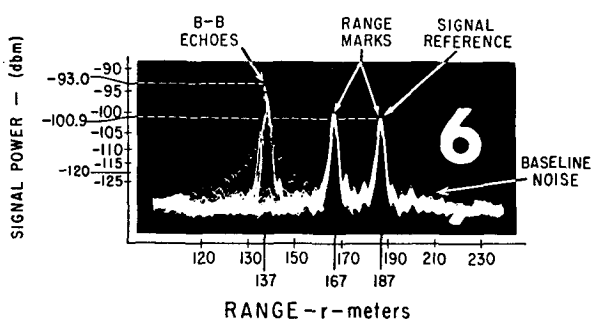

FIG. 4. Oscilloscope trace of echoes from a B-B near the top of its trajectory. Range marks and signal reference level are as indicated.

Fig. 4 is a sample of the oscilloscope trace showing the reference range and signal intensity markers and a succession of echoes from a B-B near the peak of its trajectory. Neglecting drag, it is readily shown that a B-B spends 2 sec within 4.9 m of its peak height on the way up and down. This accounts for the succession of overlapping echoes from the target at the radar repetition rate of 10 sec^{-1}. The maximum signal is used for the calibration since this is where the B-B comes closest to the beam axis. The side-lobe peaks associated with the echo traces are due to the frequency side lobes of the spectrum analyzer used in the system to translate the target beat frequency to range. The baseline noise at short ranges is due primarily to weak echoes from nearby ground clutter.

Of the 77 shots we arbitrarily selected the 22 which produced the greatest signal intensities. The echo intensity and range for each of these were read from the photographs as in Fig. 4 and the corresponding values of K calculated according to (10). Because it is not possible to attain values of K larger than that corresponding to a target on the axis of the beam, we chose the five shots having the largest K. We did not select the single largest value because the random errors,[4] mainly the result of scope and receiver calibration and reading the data points, were estimated to be about ± 2 dB. The average of the largest five was $\bar{K} = -7.3$ dB (relative to 1 mW m^4), with all five falling within -1.3 and $+1.0$ dB of the average.

Using the parameters of Table 1 with the actual transmitted power of 8.71×10^4 mW and an assumed antenna efficiency, $f = 1$ in Eq. (10), we find a theoretical maximum K of -1.17 dB (1 mW m^4). The observed K is thus -6.13 dB below the theoretical maximum, the difference being a measure of the combined antenna efficiencies f^2. Thus $10 \log f^2 = -6.13$ dB and $f = 0.493$. Using (2a) with $f = 0.493$ and G_m from Table 1, the effective axial antenna gain is 4.22×10^3. This is just 0.86 dB greater than the measured axial gain of 3.47×10^3 prior to installation. Accordingly, the B-B tests indicate that the two-way sensitivity of the system is 1.7 dB better than expected from the antenna gain measured on the antenna range. Since this is within our estimated experimental error, and it is difficult to imagine how the antenna gain in the actual installation could exceed that recorded on the antenna range, we conclude that the system is performing essentially in accord with theory. Thus, in all that follows we shall assume the values of antenna gain, efficiency and beam width recorded on the antenna range (see Table 1). Three significant figures are usually carried for purposes of consistency and not to indicate accuracy.

[4] We are confident that the error can be reduced to less than ± 1 dB by exerting greater precautions in the calibration procedure.

A similar experiment in the summer of 1969, during which we shot in excess of 100 B-B's, resulted in an effective gain of 3.16×10^3, or 0.4 dB smaller than that measured on the antenna range.

4. Internal consistency of antenna beamwidth and gain

Silver (1949) has shown that the overall efficiency of an antenna is given by

$$f=\alpha\xi, \tag{12}$$

so that the effective antenna gain G_e in (2a) is

$$G_e=\alpha\xi G_m. \tag{13}$$

Here α is the fraction of the total transmitted power intercepted by the antenna including effects of aperture blocking, and ξ the efficiency of the aperture in concentrating the available energy into the peak of the main lobe. For a well-shaped antenna, ξ depends entirely on the primary illumination pattern from the feed. In addition, Silver and others have demonstrated that the horizontal and vertical beamwidths between half-power points of the radiation pattern are given, respectively, by

$$2\theta_h=F_1(\xi)\lambda/D_1, \tag{14a}$$

$$2\phi_h=F_2(\xi)\lambda/D_2, \tag{14b}$$

where D_1 and D_2 are the antenna dimensions in the θ and ϕ directions, respectively, and $F(\xi)$ are functions of ξ, the beam concentrating efficiency. For an aperture of elliptical shape, the geometric face area $A=\pi D_1D_2/4$ so that we may combine (17a) and (17b) with the result that

$$4\theta_h\phi_h=F^2(\xi)\pi\lambda^2/(4A), \tag{15}$$

where $F^2(\xi)=F_1(\xi)F_2(\xi)$. In the case of a circular paraboloid with $D_1=D_2$ and $\theta_h=\phi_h$,

$$4\theta_h^2=F^2(\xi)\pi\lambda^2/(4A). \tag{16}$$

Noting that the maximum possible antenna gain $G_m=4\pi A/\lambda^2$, we then substitute (16) into (13), whence

$$G_e=\pi^2k^2/(4\theta_h^2), \tag{17}$$

where

$$k^2=\alpha\xi F^2(\xi)=fF^2(\xi), \tag{18}$$

and f is the overall antenna efficiency. Thus, the measurements of antenna gain, efficiency and beamwidth must be consistent with (17) and (18.)

The beamwidth measured on the antenna range is $2\theta_h=2\phi_h=2.5°$ or 4.36×10^{-2} rad at the mid-frequency of 2.90 GHz. From (14), with $\lambda=10.35$ cm and $D=3.048\times10^2$ cm, this beamwidth corresponds to $F(\xi)=1.285$. Silver (1949, p. 195, Table 6.2) gives values of ξ (which he refers to as the "gain factor") and $F(\xi)$ for circular apertures which are illuminated by primary amplitude radiation patterns from the feed of the form

$$E(x)/E(0)=(1-x^2)^p,$$

where x is the fraction of the maximum aperture radius and p takes on values from 0 to 4. The relevant portions of Silver's Table 6.2 are reproduced in Table 2.

TABLE 2. Secondary pattern characteristics produced by a primary amplitude illumination of $(1-x^2)^p$ over a circular aperture (after Silver, 1949).

p	ξ	$F(\xi)$	First side lobe (dB <peak)
0	1.00	1.02	17.6
1	0.75	1.27	24.6
2	0.56	1.47	30.6
3	0.44	1.65	
4	0.36	1.81	

Interpolation from Table 2 shows that the value of $F(\xi)=1.285$ associated with a 2.5° beamwidth implies that p is slightly greater than 1 and $\xi=0.735$. Also the first side lobe should be about 25 dB down from the main lobe intensity. In actual fact the first side lobes are somewhat smaller, but the second side lobes are about 25 dB down (see I). Taking the measured gain at 2.9 GHz, we have already seen that this corresponds to an overall antenna efficiency $f=0.405=\alpha\xi$ (Table 1). Thus with $\xi=0.735$, we find $\alpha=0.55$. This is a surprisingly small α but it is the only value which is consistent with both the measured antenna gain and beamwidth. The overall efficiency of 40% is nevertheless not excessively low for a practical antenna (McKee *et al.*, 1967).

Finally, with $f=\alpha\xi=0.405$ and $F(\xi)=1.285$, Eq. (18) results in $k^2=0.669$. This will be of use in what follows. It is important to note that this k^2 is significantly smaller than unity, the value which Probert-Jones (1962) suggests as applicable to most meteorological radars with circular paraboloids.

5. The final radar equations

a. Point targets

Using the gain and overall efficiency measured on the antenna range, the typical transmitted power of 10^5 mW, and a minimum detectable signal of 10^{-15} mW in (3), the radar equation for a point target on the effective beam axis may be shown to be

$$\sigma_{\min}\psi=3.07\times10^{-6}r^4\ [r(\text{km});\sigma(\text{cm})^2]. \tag{19}$$

With $\psi=1$ (no correction for beam intersection), (19) compares to $\sigma_{\min}\approx3.7\times10^{-6}r^4$ reported by Richter (1969). In actual fact, the minimum detectable signal is range-dependent because of the presence of irreducible echoes from nearby ground targets. Where such clutter echoes are present the minimum detectable signal is close to 10^{-14} mW, increasing the minimum detectable cross section given by (19) by a factor of about 10.

b. Distributed targets

In the case of distributed targets, Probert-Jones (1962) has shown that the radar equation is

$$\bar{P}_r=\frac{P_t A_e h\eta}{8\pi r^2}L\left(\frac{\pi^2 k^2}{32\ln 2}\right)\psi, \tag{20}$$

where the quantities have their previous meanings except that $\bar{P}_r$ is the average echo power returned from the ensemble of scattering elements, and η is the cross section per unit volume or the reflectivity of the scatterers and is assumed constant across the beam and along the effective pulse depth in space, $h/2$. It is implicit in (20) that $h/2 \ll r$. We have also multiplied Probert-Jones' original equation by the range correction factor ψ which we have shown in I is identical to (7a). In addition, the quantity k^2 is defined by (17) or (18).

Inserting the appropriate values from Table 1, $k^2=0.669$ and $P_r(\min)=10^{-15}$ mW into (20), we find

$$\eta_{\min}=5.72\times10^{-15}r^2/(h\psi)\ \ [\eta(\mathrm{cm})^{-1};r(\mathrm{km});h(\mathrm{m})]. \tag{21}$$

The coefficient in (21) may be compared to the value 4.2×10^{-15} given by Richter (1969).

6. Summary and conclusions

In order to calibrate a dual-beam vertically pointing FM-CW radar, we have fired B-B's from a CO_2-powered air pistol. The B-B's are used as standard targets of known cross section. A large number of shots are required with successive adjustments in trajectory in order to ensure that at least a few of the B-B's cross the maximum of the combined beam. The technique is simple, quick and cheap, and yielded an effective antenna gain within 0.9 dB of that measured on an antenna range. The radar is therefore performing in very close accord with theory. Because the FM-CW radar permits the target range to be measured with great accuracy ($\pm\frac{1}{2}$ m) at ranges of 130–150 m, the calibration error is essentially that associated with the measurement of the ratio of received to transmitted power, and reading inaccuracies, about ±2 dB in the present experiment. The error can surely be reduced to less than ±1 dB by exerting greater care in the calibration procedure. A correction to the radar equation for both point and distributed targets is included for the effect of displaced beam axes at ranges other than that at which the axes intersect. Radar-range equations appropriate to the radar both for point and distributed targets are presented. It is also found that Probert-Jones' (1962) k^2 factor is significantly smaller than the previously recommended value of unity.

The method can be readily adapted to any pulsed radar such as the AN/CPS-9 which can detect B-B shot at short ranges. In such a case the range to the firing point should be measured directly rather than by the radar in order to avoid the excessive range errors possible with relatively long pulses. Also, a direction should be chosen where the ground clutter echoes at small beam elevation angles (e.g., about 7 or 8° at 1 km range for B-B's reaching 140 m) are at least 10 dB smaller than the echo expected from the B-B.

Acknowledgments. Messrs. Stratmann and Atlas are indebted to Dr. Earl E. Gossard, Head, Propagation Technology Division, Naval Electronics Laboratory Center, San Diego, for arranging for our use of the radar. We also appreciate the assistance of Messrs. W. K. Horner, D. W. Truax and L. D. Duncan, of NELC, in conducting the experiments.

This investigation was supported in part by Research Grant DA-ARO-D-31-124-71-G71, U. S. Army Research Office–Durham, by Research Grant 1-R01 AP-01369-01, Air Pollution Control Office, Environmental Protection Agency, and by a grant from the United Airlines Foundation.

REFERENCES

Atlas, D., and K. R. Hardy, 1966: Radar analysis of the clear atmosphere: Angels. *Proc. XV General Assembly, URSI*, 401–469.

——, F. I. Harris and J. H. Richter, 1970a: The measurement of point target speeds with incoherent non-tracking radar: Insect speeds in atmospheric waves. Tech. Rept. No. 17, Laboratory for Atmospheric Probing, The University of Chicago, 31 pp.

——, J. I. Metcalf, J. H. Richter and E. E. Gossard, 1970b: The birth of "CAT" and microscale turbulence. *J. Atmos. Sci.*, **27**, 903–913.

Hardy, K. R., and I. Katz, 1969: Probing the clear atmosphere with high power, high resolution radars. *Proc. IEEE*, **57**, 468–480.

Kerr, D. E., 1951: *Propagation of Short Radio Waves*. MIT Radiation Laboratory Series, Vol. 13, New York, McGraw-Hill, 445–453.

Lane, J. A., 1968: Small-scale variations of radio refractive index in the troposphere. Part 1: Relationship to meteorological conditions. *Proc. IEE (London)*, **115**, 1227–1234.

McKee, K. E., A. G. Holtum, Jr. and T. E. Charlton, 1967: Optimizing gain of parabolic antennas. *Microwaves*, March, 34–39.

Probert-Jones, J. R., 1962: The radar equation in meteorology. *Quart. J. Roy. Meteor. Soc.*, **88**, 485–495.

Richter, J. H., 1969: High-resolution tropospheric radar sounding. *Radio Sci.*, **4**, 1261–1268.

Silver, S., 1949: *Microwave Antenna Theory and Design*. MIT Radiation Laboratory Series, Vol. 12, New York, McGraw-Hill, p. 199.

Skolnik, M. I., 1970: *Radar Handbook*. New York, McGraw-Hill, 1.4–1.8.

Stratmann, E., D. Atlas, J. H. Richter and D. R. Jensen, 1971: Sensitivity calibration of a dual beam vertically pointing FM-CW radar. Tech. Rept. No. 21, Laboratory for Atmospheric Probing, University of Chicago and Illinois Institute of Technology, 26 pp.